Large-scale Rossby wave and synoptic-scale dynamic analyses of the unusually late 2016 heat wave over Europe

Journal:	*Weather*
Manuscript ID	WEA-17-0109.R1
Wiley - Manuscript type:	Research Article
Date Submitted by the Author:	n/a
Complete List of Authors:	Zschenderlein, Philipp; Karlsruher Institut für Technologie, Institute of Meteorology and Climate Research Fragkoulidis, Georgios; Johannes Gutenberg Universität Mainz, Institute of Atmospheric Physics Fink, Andreas; Karlsruher Institut fur Technologie, Institute of Meteorology and Climate Research Wirth, Volkmar; Johannes Gutenberg Universität Mainz, Institute of Atmospheric Physics
Keywords:	Heat waves, Rossby Waves, Lagrangian trajectory analysis, Adiabatic and diabatic temperature changes
Comprehensive Country List:	

Large-scale Rossby wave and synoptic-scale dynamic analyses of the unusually late 2016 heat wave over Europe

Philipp Zschenderlein[1*], Georgios Fragkoulidis[2], Andreas H. Fink[1], and Volkmar Wirth[2]

[1] Karlsruhe Institute of Technology, Institute of Meteorology and Climate Research, Karlsruhe, Germany

[2] Johannes Gutenberg University, Institute of Atmospheric Physics, Mainz, Germany

[*] Corresponding author: Philipp Zschenderlein, Karlsruhe Institute of Technology, Institute of Meteorology and Climate Research, Kaiserstr. 12, 76128 Karlsruhe, Germany. E-mail: philipp.zschenderlein@kit.edu

Abstract

This paper analyses the late summer heat wave over Europe in 2016. Primarily central, western and southwestern Europe were affected by high temperatures. Seville (Spain), for example, registered the highest September temperature on record on 5 September 2016 topping at 44.8°C, as well as Trier with temperatures reaching 34.2°C on 13 September 2016. The heat wave was marked by three distinct peaks, accompanied by record-breaking values of 500-hPa geopotential heights and, to a lesser extent, 850-hPa temperatures. These peaks were associated with the arrival of high-amplitude Rossby wave packets in western Europe. The latter originated several days before the event over western North America. During the three peaks of the heat wave, subsidence and ensuing adiabatic compression in the free atmosphere in combination with boundary layer processes rather than local temperature advection were instrumental in the occurrence of the extreme temperatures.

Keywords: Heat waves, Rossby waves, Lagrangian trajectory analysis, adiabatic and diabatic temperature changes

Introduction

Among the robust statements in the 5th IPCC (Intergovernmental Panel on Climate Change) report was that heat waves in Europe will be more frequent and intense at the end of the 21st century (Collins et al., 2013). Observations show an accelerated warming of mean surface temperatures over Europe since the middle of the 20th century and observational studies hint at an already elevated probability of heat waves in this region (Hartmann et al., 2013). Notable recent heat waves with large

socio-economic impacts that struck western Europe and Russia occurred in summer 2003 and 2010, respectively (Fink et al., 2004; Russo et al., 2015; Quandt et al., 2017). There exists a diversity of studies on heat waves and the role of soil moisture anomalies on seasonal and climate time scales (e.g. Fischer et al., 2007), but fewer studies investigated the dynamical development and the predictability of heat waves (e.g. Black et al., 2004; Miralles et al., 2014; Bieli et al. 2015; Quandt et al., 2017). Heat waves are often associated with the development of ridging or blocking in the upper-level flow several days prior to the events that can be related to Rossby wave dynamics (e.g. Fink et al., 2004, Pfahl and Wernli, 2012, Fragkoulidis et al. 2018). Without these large-scale precursors, a heat wave is unlikely to occur despite pre-existing desiccated soils. Under similar large-scale ridging characteristics persisting one to three days prior to peak temperatures, synoptic and meso-scale boundary layer processes shall then be more important to determine the exact value of the maximum temperature at a weather station. The present study seeks to shed light both on the large-scale Rossby wave behaviour and the local processes contributing to the three peaks of a heat wave that affected southwestern, western and central Europe in late summer and early autumn 2016. The role of the local processes, viz. horizontal temperature advection, adiabatic compression by subsidence and heat fluxes, will be investigated. These are all terms of the Eulerian form of the temperature tendency equation (Carlson, 1994). The Rossby wave packets will be traced back over the Atlantic using an appropriate diagnostic proposed by Fragkoulidis et al. (2018).

The 2016 late summer season heat wave is remarkable in that it sets the stage for the development of the first-ever reported tropical-like storm in the Bay of Biscay at their end (Maier-Gerber et al. 2017). The authors noted the record-breaking sea surface temperatures (SSTs) in the Gulf of Biscay that were the consequences of calm, sunny, and warm weather in the weeks leading to the “Biscane” (by analogy with Medicanes as “Mediterranean hurricanes”) named “Stephanie” on 15 September 2016. Figure 1(a) shows the ERA-Interim (cf. Dee et al., 2011) based time series of daily maximum 2-metre temperature averaged between 35°-55°N and 11°W-15°E (cf. rectangle in Figure 1(b)) for June to September 2016 in comparison with the daily climatology for 1979-2016. The 2016 summer was characterized by several short warm periods, especially in June and July. Towards the end of the summer season, a heat wave commenced around 23 August and lasted until the middle of September. With three peaks occurring around 23 August, 05 and 13 September, mid-summer temperature levels were preserved against the large climatological temperatures decrease (green dashed line in Figure 1(a)). As a consequence, the temperature anomalies steadily increased. Based on a commonly used, temperature-based heat wave index discussed in the next section, the largest positive temperature anomalies were observed in Spain, central and western Europe (Figure 1(b)). Bordeaux in southwestern France registered a maximum daily temperature of 37°C during the first

peak on 23 August 2016. The second peak was record-breaking, especially for southern Spain. Seville measured 44.8°C, which was the highest temperature on record for any September month at this station. The last peak affected mainly central Europe, where for example Trier measured 34.2 °C on 13 September 2016, which was also the highest temperature on record for any September month at this station. For the location of the three stations the reader is referred to Figure 2. In the following sections, details will be given on the magnitude of the heat wave, its evolution in the upper-troposphere, and on the relative roles of temperature advection, subsidence and boundary layer heat fluxes to explain the temperature extremes at the three above-mentioned European cities.

Magnitude of the heat wave

In order to quantify the onset, termination, and magnitude of the heat wave, we applied the percentile-based heat index (Heat Wave Magnitude Index daily, HWMId) after Russo et al. (2015). According to their definition, a heat wave is a period of at least three consecutive days for which the daily maximum temperature exceeds the 90th percentile of a 31-day period centred on this day. The magnitude of the heat wave is then determined in two steps. First the difference between the daily maximum temperature and the 75th percentile of annual maximum temperatures, normalised by the interquartile range, is calculated for each heat wave day. Then these values are summed up over the whole heat wave period at each grid point leading to its HWMId value (Figure 1(b)). In view of the climatological temperature decrease towards the end of August and during September (Figure 1(a)), we had to adjust the reference period used to calculate the heat index. More specifically, we only considered annual maximum temperatures between 15 August and 30 September 1981-2010 as a climatological reference. Figure 1(b) shows the HWMId sum for the identified heat wave period between 23 August and 16 September for 2-metre temperatures. Contrary to Russo et al. (2015), the index was calculated both over land and ocean. Hence, positive values above land surfaces indicate high surface temperatures, whereas positive values above the oceans indicate high SSTs due to their strong influence on 2-metre temperatures. Central and western Europe were particularly affected during the first and the last peak, whereas the second peak was very intense for Spain, thus resulting in the cumulative heat index displayed in Figure 1(b). Adjacent waters showed also high values of HWMId, especially parts of the Bay of Biscay, the Gulf of Cadiz and Lions, and the North and the Baltic Seas. Note that in the North Sea, for the first time since observations started in 1968, the highest SSTs were recorded in September instead of August (BSH, 2016). Compared to the 2003 heat wave mentioned in the Introduction, the spatial extent in 2016 is comparable, whereas HWMId values were smaller in that year (not shown). Note that this can be due to differences in both magnitude and duration of the heat waves.

The HWMId index can also be applied to temperature at 850 hPa (not shown). While on overall similar spatial pattern emerged, higher values at 850 hPa occurred over the UK and the North Sea, indicating that the maritime climate of the British Isles dampened the warmth at the surface.

Synoptic evolution

In this section, the spatio-temporal evolution of the heat wave from a synoptic perspective is presented. The first peak of the heat wave on 23 August 2016 was associated with an extremely strong 500-hPa ridge that extended from the Iberian Peninsula across central Europe to the southern parts of Scandinavia. The maximum geopotential height value of approximately 596 gpdam was near the Pyrenees. As can be inferred from the pink shading in Figure 3(a), over large parts of west and southwest Europe the highest geopotential height values in the period 1979-2016 were recorded on this day for this time of the year. All percentiles in Figure 3 for a particular day were calculated with respect to a centred 21-day window (only 1200 UTC), spanning the years 1979-2016. Eastern France recorded even the highest geopotential height since 1979. Although not as extreme as the geopotential height values, temperatures at 500 hPa (Figure 3(b)) were also very high, with values above the 95th percentile covering much of western Europe. At the western flank of the ridge, extremely high temperatures dominated at 850 hPa (Figure 3(c)), with values exceeding 22°C over France. At this time of the year, such high temperatures are very unusual poleward of 40°N in western Europe and correspond to the top 1% of the climatological distribution (red areas in Figure 3(c)). The upper level ridge propagated eastward during the next few days, thereafter the flow became more zonal and the heat wave weakened. The second peak of the late summer warmth affected Spain and evolved under a strong ridge extending over southwestern Europe. Similar to the first peak, a large area surpassed the highest geopotential height values on record (Figure 3(d)), with a maximum of 599 gpdam in southern Spain. However, this time the region was displaced to the southwest and was located over Spain and northern Morocco. Contrary to the first peak, both temperatures at 500 and 850 hPa reached record values too (Figures 3(e) and (f)), though the areas were not as large and contiguous as for the geopotential height. Small areas of record-breaking temperatures at 850 hPa were observed over Ireland and southeastern Spain with absolute values of 17°C and 26°C, respectively. As a consequence, the thermal tropopause, derived from sounding data in Murcia (Spain), reached altitudes of about 15 km (not shown), which is reminiscent of tropical air masses. The final peak of the heat wave was related to an “Omega-type” blocking with the ridge centred over central Europe and Scandinavia. The ridge pattern was similar for antecedent days, thereby interrupting the prevailing westerlies over central Europe, a situation that favours hot extremes (Pfahl and Wernli, 2012). While 500-hPa geopotential height and temperature values on 13 September 2016 were by far less extreme than during the previous two heat peaks (Figure 3(g), and

(h)), the 850 hPa temperatures were extreme under the westerns flank of the ridge over northwestern Europe and Scandinavia, with values over the British Channel and North Sea (above 18°C) being the highest in the reference period (Figure 3 (i)). Finally, it shall be noted that the elongated trough extending down to the western Iberian Peninsula later developed into a cut-off low over the Bay of Biscay the led to the development of the Biscane "Stephanie" (Maier-Gerber et al., 2017).

Large-scale atmospheric precursors

Next, we present a large-scale perspective of the heat wave by trying to depict the upstream development of the Rossby wave packets (RWPs) in which the ridges described in the previous section were embedded. A large amplitude RWP can be considered as the envelope encompassing a series of high amplitude ridges and troughs in the upper-level flow. RWPs have been shown to be relevant for surface weather (Wirth et al., 2018). Figure 4 shows maps of anomalous meridional wind v' (the prime denoting anomalies from the de-trended 1979-2016 mean, see Fragkoulidis et al. (2018) for details) at 300 hPa, temperature T' at 850 hPa and geopotential height at 300 hPa for the three days corresponding to the three peaks in Figure 1(a). In all cases, waviness at 300 hPa over the North Atlantic/Europe region was apparently high. Deep 300-hPa troughs upstream of Europe were marked by strong southerly winds at their eastern flanks, with the 850-hPa temperature anomalies being located farther downstream of the wind maxima (Figure 4). The time evolution of the RWP can be studied using a refined RWP diagnostic described in Fragkoulidis et al. (2018) that allows to track zonally constrained wave packets propagating eastward in a self-adjusting latitude band instead of assessing the Rossby waviness along an entire latitudinal circle using Fourier analysis.

The left panel of Figure 5 shows a circumglobal Hovmoeller diagram for the period mid-August to mid-September 2016 with the 300-hPa RWP amplitudes as contours and meridional wind anomalies v' as colour fill. In addition, the right panel of Figure 5 shows the normalised temperature anomalies T' at 850 hPa (red line) averaged over 35°-55°N and 11°W-15°E, highlighting in orange the exceedances of the August-September 90th percentile (blue dashed line). Apparently, three successive periods of extremely high temperatures occurred over Europe between 23 August and 14 September 2016. All these periods coincided with strong signals of upper-tropospheric waviness, associated with series of strong meridional wind anomalies embedded in the larger scale RWPs. The meridional wind anomalies mark the troughs and ridges embedded in the RWP. These RWPs formed over western North America (at around 120°W), propagated eastward with a group velocity (cf. green arrows in left panel of Figure 5) on the order of about 30° longitude per day. This is faster than the phase speed of the embedded troughs and ridges that can be inferred from the propagation

speed of the meridional wind anomalies. The RWPs acquired their maximum amplitude over the North Atlantic Ocean. Their arrival to Europe concurred with the aforementioned hot periods. Large amplitude ridges in all three cases provided a favourable environment for the smaller-scale processes that led to warming in the investigated locations (see next section). Finally, after the dispersion of the RWPs, the warm air masses were not sustained and short periods of mild temperatures provided relief to the affected areas.

Figure 5 clearly reveals that the enhanced atmospheric upper-level waviness is a mid-latitude propagating phenomenon that can be traced back upstream a few days before the event and is initiated several thousand or, as for the second heat wave with a potential precursor in the Pacific Ocean, more than 10,000 km to the west of Europe. The related large-, sometimes even planetary-scale Rossby wave dynamics suggests relative high predictability – and indeed at lead times of a few days, the 51 members of the ECMWF ensemble prediction system shifted towards positive anomalies for Bordeaux, Seville, and Trier, indicating increasing probabilities of an imminent heat wave at the respective locations (not shown). A similar observation is mentioned in Magnusson et al. (2015) for a heat wave affecting Paris (France) in July 2015. However, the spatio-temporal details on the extent of the warmth ultimately depend on the phase velocity and amplitudes of the Rossby waves, i.e., the trough ridge systems embedded in the RWP (see discussion in Fragkoulidis et al., 2018 for the 2003 and 2010 European heat waves), as well on the related temperature advection, subsidence and heat fluxes in the boundary layer. The role of the latter two processes will be discussed in the next section.

BOX 1: T-Θ Diagram

The purpose of the T-Θ phase diagram (Scheme 1) is to distinguish adiabatic from diabatic temperature changes experienced by an air parcel following its motion (Bieli et al., 2015). The diagram depicts both the temperature T (y-axis) and the potential temperature Θ (x-axis) of an air parcel and its possible changes. The potential temperature Θ is the temperature that an air parcel would attain when it was moved adiabatically to 1000 hPa. Adiabatic processes are defined as processes that do not change the dry entropy of an air parcel, which implies that the potential temperature is materially conserved following the motion and that changes occur reversibly. Diabatic processes, in contrast, are associated with an exchange of energy between an air parcel and its environment, resulting in an irreversible material rate of change of the potential temperature. Examples for a diabatic process include radiative processes, subgrid-scale turbulent fluxes (especially in the boundary layer) and the release of latent heat due to phase changes in clouds. For illustration,

the reader should imagine an air parcel located at the origin of the arrows, as marked with a grey circle (Scheme 1). Movements in the strictly vertical direction of the T-Θ Diagram indicate adiabatic processes since Θ is conserved. By contrast, diabatic processes occur for all non-strictly vertical displacements of the parcel in the T- Θ diagram with the red (blue) semicircles indicating diabatic heating (diabatic cooling). The parcel may undergo the following changes: Increasing T due to subsidence (compression of the air parcel, adiabatic warming) indicated by the upward pointing arrow towards letter "A"; decreasing T due to lifting (expansion of the air parcel, adiabatic cooling) indicated the downward pointing arrow towards "C"; increasing Θ due to diabatic warming, but at the same time decreasing T, which can only be explained by lifting and, hence, adiabatic cooling overcompensating the diabatic heating (quadrant "B2"); decreasing Θ due to diabatic cooling, but at the same time increasing T, which can only be explained by subsidence and, hence, adiabatic warming overcompensating the diabatic cooling (quadrant "D1"); the quadrants "B1" ("D2") are associated with diabatic heating (cooling), respectively, but no conclusion can be drawn regarding the vertical motion.

Development of high temperature extremes near the surface

In this section, we will address the following questions: (i) where do the hot air masses originate, (ii) which physical processes contribute to the high temperature extremes at the observation stations, and (iii) does the heat propagate from upper levels to the surface or vice versa? To achieve an answer to these questions, we use the Lagrangian trajectory analysis tool developed by Wernli and Davies (1997). We computed 5-day backward trajectories from six-hourly ERA-Interim wind fields. Trajectories were only started above the three cities if temperatures in the lower and middle tropospheric levels exceeded the 95th percentile of the temperature distribution on 23 August, 05 and 13 September 2016, respectively.

Figure 6(a) shows 5-day backward trajectories, starting on 23 August 2016, 1200 UTC between 975 and 550 hPa over Bordeaux (note that trajectories at the surface in this three-dimensional plot are the projection of the upper-air trajectories, with both having the same colour). Almost all trajectories arriving at Bordeaux on 23 August 2016 crossed the North Atlantic Ocean between 800 and 500 hPa, i.e. above the marine boundary layer. Near Europe and 48 hours before the event, the air parcels strongly descended along an anticyclonic trajectory to approach Bordeaux from the northeast, i.e. from a direction for which they travelled a long time over land, experiencing clear-sky conditions (not shown). The T-Θ phase diagram (Figure 6(b)), see Box 1 for explanation) clearly discloses that the air parcels, especially arriving at lower levels over Bordeaux, experienced a

substantial increase in temperature by 20-25°C due to adiabatic compression 48 hours prior to the event. The temperature increase is close to adiabatic as indicated by the very small rate of change of the parcels' potential temperature during this stage (Figure 6(b)). Apparently, this adiabatic warming is consistent with the subsidence visible in Figure 6(a). Just before the extreme event, the trajectories closest to the surface experienced slight diabatic warming (red line in Figure 6(b)), presumably due to turbulent heat fluxes from the surface, as they were transported above land surfaces (Figure 6(a)). Figure 6(c) shows the development of temperature anomalies between 18 and 23 August in the lower and mid-troposphere above Bordeaux from an Eulerian perspective. Between 90 and 36 hours before the peak temperatures were reached on 23 August 2016 1200 UTC, the atmosphere was comparably cold, especially between 900 and 800 hPa. The temperatures increased rapidly before the actual extreme event. Interestingly, the positive anomalies initiated at higher levels and penetrated subsequently to the surface. Hence, the temperature anomalies "propagate" downward. The propagation is consistent with the subsidence, which is remarkably high in the last 36 h prior to the hot extreme. Overall, this suggests that subsidence and adiabatic compression are the driving factors in establishing the high temperatures at the surface. Figure 6(d) shows diurnal cycles (0600, 1200, 1800 UTC) of vertical profiles of virtual potential temperature Θ_v for the pre-heat wave (18 August 2016, dashed) and the heat wave period (23 August 2016, solid). The profiles unravel (a) the strong lower tropospheric warming between 18 and 23 August 2016, (b) a quite constant and shallow depth of the well-mixed (i.e. Θ_v nearly constant with height) boundary layer and (c) a strong diurnal cycle on the hot 23 August 2016.

Figure 7 shows the same set of panels as in Figure 6 for the hottest September day on record in Seville on 5 September 2016. Backward trajectories are only started up to 700 hPa, because at higher altitudes the temperatures were not extreme (cf. Figure 7(c)). Compared to Bordeaux, the air parcels travelled a much shorter distance during the five days preceding the heat wave. Although most of the trajectories had an anticyclonic curvature, the individual origins of the air parcels were however diverse. Parcels which ended up near the surface in Seville originated in northern Spain, those ending up at higher altitudes over Seville had their origins mostly over the warm northern Africa; a pathway that was favoured by the large-scale setting to the North (RWP) and realized in connection with a short upper-level trough to the southwest of the Iberian Peninsula (Figure 4(b)). Nearly all trajectories entered the Seville area from the east. Parcels arriving near the surface warmed adiabatically in the last 72 h by about 30°C (Figure 7(b)). They experienced subsidence over a longer time period (3 days) than those over Bordeaux (2 days). Again, this suggests that subsidence contributed significantly to this hot event. Interestingly, the air parcels starting between 700 and 775 hPa in Seville warmed diabatically 48 to 24 h before the event. This took place in the surroundings of

the Atlas Mountains (Figure 7(a)), which suggests that turbulent heat fluxes and moist convection in this area played an important role. A more detailed analysis of the diabatic processes (including cloud-microphysics) is beyond the scope of this study. Figure 7(c) shows the vertical structure of the atmosphere over Seville from 31 August to 5 September. Striking is the completely different behaviour of this heat event compared to the former case. Distinct positive temperature anomalies developed 48 h prior the extreme event with a maximum at the surface and the lower tropospheric layers. Compared to the lower planetary boundary layer heights five days before the high temperature event in Seville, the boundary layer deepened during the heat event. This can be inferred from the near constant vertical profile of Θ_v in Figure 7(d). Black et al. (2004) found also elevated planetary boundary layer heights above Paris during the 2003 heat wave. It appears that strong solar insolation, ensuing surface fluxes and dry convection deepened the boundary layer. The evolution of the temperature profiles indicates a bottom-up development similar to the findings of Miralles et al. (2014). Thus, adiabatic compression worked in concert with boundary layer processes to create the hottest September day ever recorded in Seville. Despite the suggested importance of subsidence and boundary layer processes, they cannot be considered as independent from the RWP. The large ridge embedded in the RWP was instrumental in steering the parcels toward the Seville region on anticyclonic trajectories and the clear-sky conditions.

Yet another picture emerged as the explanation for the hottest September day on record at Trier on 13 September 2016. Most of the trajectories, started from 975 up to 800 hPa where temperature extremes were present over Trier, originated near the Rhône valley and northern Italy (Figure 8(a)), yielding a horizontal transport over comparably short distances and above land surfaces only. The lowest trajectories were trapped in the planetary boundary layer, suggesting significant interaction with the land surface presumably due to enhanced surface heat fluxes. This can be seen in Figure 8(b) as an increase of the potential temperature of approximately 10 K (diabatic heating). The fluctuating temperature in Figure 8(b) indicates the diurnal temperature variation. Note, that the diurnal temperature variation is also clearly visible in Figure 8(c), as the lowest temperature anomalies were always attained at 0600 UTC near the surface. In general, the temperature increase of air parcels in Figure 8(b) was smaller compared to the aforementioned cases. Additionally, subsidence from higher levels was not observed. Rather, heat was trapped in the planetary boundary layer and accumulated day by day (Figure 8(c)), leading to an increase in the boundary layer top over Trier (Figure 8(d)). The boundary layer top was quite high for this location and late time of the year. Figure 8(c) also revealed positive temperature anomalies above Trier up to 500 hPa from 8 – 13 September. We conclude that the main reason in establishing the heat event for Trier are diabatic processes in the planetary boundary layer, e.g. heating due to upward directed surface sensible heat

fluxes caused by strong solar insolation over several days, both experienced by the parcels reaching Trier and locally over Trier.

Conclusions

We analysed the planetary- and synoptic-scale developments that led to the 2016 European late summer/ early autumn heat wave. Central, western and southwestern Europe were the most affected regions, with partly record-breaking maximum temperatures. Seville and Trier registered both the highest September temperature (44.8 and 34.2°C respectively) since the beginning of the record, which goes back to 1951 for Seville and 1941 for Trier. The three peaks were all accompanied by pronounced 500-hPa ridges. The first two peaks showed larger areas with the highest values of geopotential height for that time of the year since at least 1979. The ridges were embedded in eastwards propagating, high-amplitude Rossby wave packets arriving in western Europe. The packets had their origins over western North America. Though not discussed, local temperature advection did not play a noticeable role in local temperature changes at the three locations investigated, i.e., Bordeaux, Seville and Trier. On the contrary, the adiabatic compression term due to subsidence was exceptionally high for the Bordeaux and Seville cases. Material changes in temperature of subsiding parcels arriving at the lower troposphere at these locations were 20-30°C in 2-3 days prior to the peak of the heat waves. Diabatic processes (such as surface sensible heat fluxes due to enhanced solar insolation) and dry convection in the boundary layer appeared to be the major explanation in the case of Trier, where hardly any subsidence occurred.

The results presented in this study have potential ramifications for investigating the predictability of heat waves. While dry soils are the prerequisite of heat waves, Rossby wave dynamics may allow early alerts of an imminent heat wave (cf. Magnusson et al. 2015). In the present cases, the ECMWF ensemble prediction system indicated an enhanced likelihood of heat waves up to five days in advance (not shown), likely related to the discussed origin of the Rossby wave packets thousands of kilometres upstream. However, the final magnitude of the heat wave seems to be related to the (thermo-)dynamics details associated with the ridge embedded in the Rossby wave packet. The absolute predictability (i.e. whether the observed maximum temperature was well forecasted) of the hottest day at a few days' lead time was best for Bordeaux, followed by Seville and Trier. However, with respect to the model climatology, the ensemble prediction system showed the highest probabilities for extreme temperatures for Trier earlier, followed by Seville and Bordeaux (not shown). The role of the large-scale Rossby wave vs. synoptic and mesoscale dynamics for the ensemble predictability of heat waves at about one week to 24-hour lead times are currently investigated in the large German weather research initiative "Waves to Weather"

(http://wavestoweather.de) that is endorsed by the WMO HIWeather initiative (https://www.wmo.int/pages/prog/arep/wwrp/new/high_impact_weather_project.html). The latter aims at improving resilience to high impact weather by, amongst others, improve probabilistic forecasts. With CMIP6 global and regional climate models having much higher spatial resolution, the discussed large and synoptic-scale dynamic processes can also be meaningfully analysed for heat waves at the end of the 21st century.

Bibliography

Bieli M, Pfahl S, Wernli H. 2015. A Lagrangian investigation of hot and cold temperature extremes in Europe. *Q. J. R. Meteorol. Soc.,* **141**: 98-108. doi:10.1002/qj.2339

Black E, Blackburn M, Harrison G *et al.* 2004. Factors contributing to the 2003 European heatwave. *Weather,* **59:** 217-223. doi: 10.1256/wea.74.04

BSH, 2016. Press release of the Federal Maritime and Hydrographic Agency of Germany: Record warmth left its mark in the North Sea (in german), Source: http://www.bsh.de/de/Das_BSH/Presse/Pressearchiv/Pressemitteilungen2016/Pressemitteilung17-2016.pdf, last accessed: 30 Nov. 17

Carlson, TN. 1994. Mid-latitude Weather Systems. *Routledge, New York*, 507 pp.

Collins M, Knutti R, Arblaster J *et al.* 2013: Long-term Climate Change: Projections, Commitments and Irreversibility. In: Climate Change 2013: The Physical Science Basis. Contribution of Working Group I to the Fifth Assessment Report of the Intergovernmental Panel on Climate Change [Stocker, T.F., D. Qin, G.-K. Plattner, M. Tignor, S.K. Allen, J. Boschung, A. Nauels, Y. Xia, V. Bex and P.M. Midgley (eds.)]. *Cambridge University Press, Cambridge, United Kingdom and New York, NY, USA*

Dee D, Uppala S, Simmons A *et al.* 2011**.** The ERA-Interim reanalysis: Configuration and performance of the data assimilation system. *Q. J. R. Meteorol. Soc.,* **137**: 553–597. doi: 10.1002/qj.828

Fink AH, Brücher T, Krüger A *et al*. 2004. The 2003 European summer heatwaves and drought – synoptic diagnosis and impacts. *Weather,* **59:** 209-216. doi: 10.1256/wea.73.04

Fischer EM, Seneviratne SI, Vidale PL *et al.* 2007. Soil moisture-atmosphere interactions during the 2003 European summer heatwave. *J. Clim.*, **20**: 5081-5099. doi:10.1029/2006GL029068

Fragkoulidis G, Wirth V, Bossmann P *et al.* 2018. Linking Northern Hemisphere temperature extremes to Rossby wave packets. *Q. J. R. Meteorol. Soc.,* doi:10.1002/qj.3228

Hartmann DL, Klein Tank AMG, Rusticucci M *et al.* 2013: Observations: Atmosphere and Surface. In: Climate Change 2013: The Physical Science Basis. Contribution of Working Group I to the Fifth Assessment Report of the Intergovernmental Panel on Climate Change [Stocker, T.F., D. Qin, G.-K. Plattner, M. Tignor, S.K. Allen, J. Boschung, A. Nauels, Y. Xia, V. Bex and P.M. Midgley (eds.)]. *Cambridge University Press, Cambridge, United Kingdom and New York, NY, USA*

Magnusson L, Thorpe A, Buizza R *et al.* 2015. Predicting this year's European heat wave, *ECMWF Newsletter,* 145, 4-5

Maier-Gerber M, Pantillon F, Di Muzio E *et al.* 2017. Birth of the Biscane, *Weather*, **72:** 236-241. doi:10.1002/wea.2995

Miralles DG, Teuling AJ, van Heerwaarden, CC *et al.* 2014 Mega-heatwave temperatures due to combined soil desiccation and atmospheric heat accumulation, *Nature Geosc.,* **7**: 345-349. doi: 10.1038/NGEO2141

Pfahl S, Wernli, H. 2012. Quantifying the relevance of atmospheric blocking for co-located temperature extremes in the Northern Hemisphere on (sub-)daily time scales, *Geophys. Res. Lett.,* **39:** L12807. doi:10.1029/2012GL052261

Quandt LA, Keller JH, Martius O *et al.* 2017. Forecast variability of the Blocking System over Russia in Summer 2010 and Its Impact on Surface Conditions. *Wea. Forecasting,* **32:** 61-82. doi: 10.1175/WAF-D-16-0065.1

Russo S, Sillmann J, Fischer EM 2015. Top ten European heatwaves since 1950 and their occurrence in the coming decades. *Environ. Res. Let.,* **10:** 1-15. doi: 10.1088/1748-9326/10/12/124003

Wirth V, Riemer M, Chang EKM *et al.* 2018. Rossby Wave Packets on the Mid-Latitude Rossby Waveguide - a Review. Submitted to *Mon. Wea. Rev.*

Wernli H, Davies HC. 1997. A Lagrangian-based analysis of extratropical cyclones. I: The method and some applications. *Q. J. R. Meteorol. Soc.,* **123:** 467-489. doi: 10.1002/qj.49712353811

Acknowledgements

The research leading to these results has been done within the subproject *C4: Coupling of planetary-scale Rossby wave trains to local extremes in heat waves over Europe* of the Transregional Collaborative Research Center SFB / TRR 165 "Waves to Weather" funded by the German Research Foundation (DFG). We are very thankful to Stephan Pfahl and Heini Wernli (both ETH Zurich) for inspiring discussions. We also thank two anonymous reviewers and the editor for their valuable comments that undoubtedly helped to improve the manuscript.

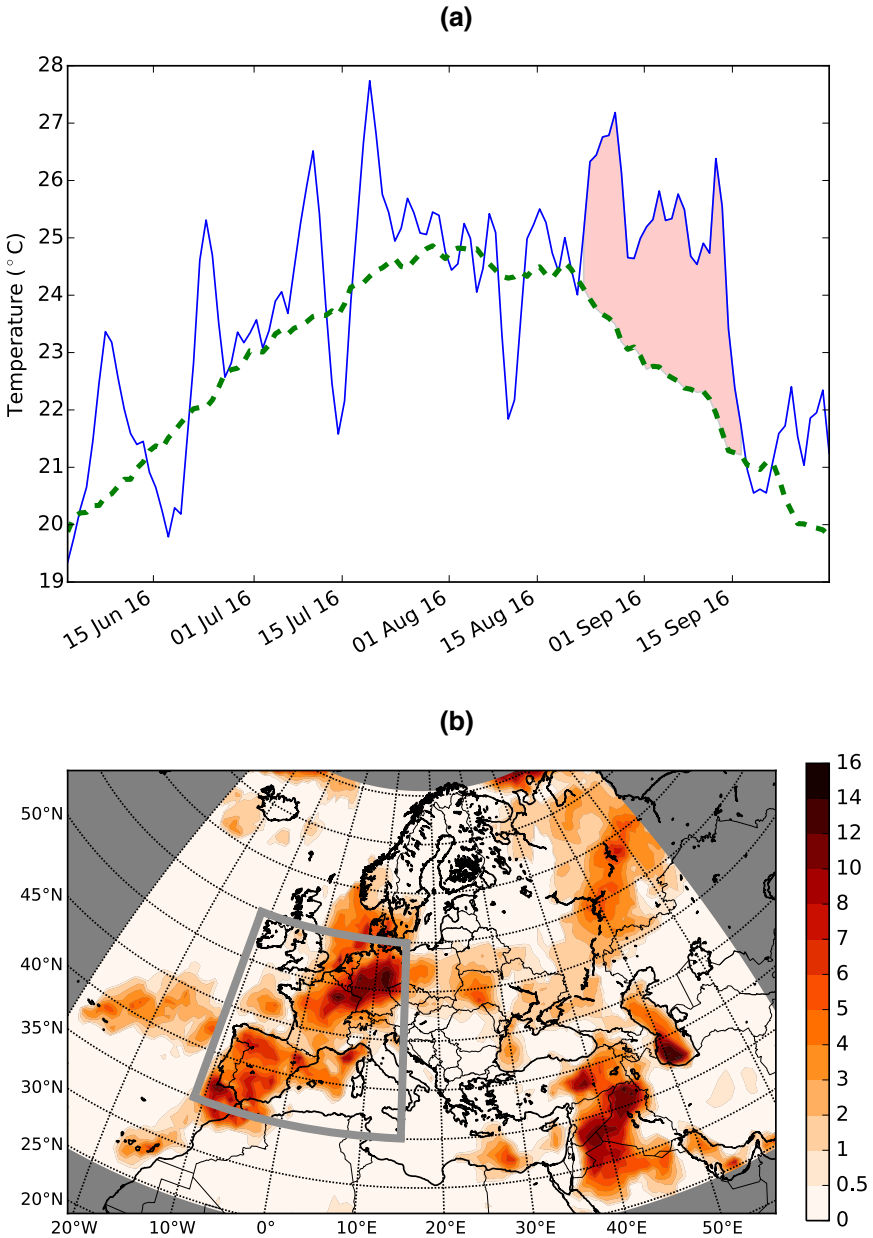

Figure 1. Spatio-temporal extent of the late summer heat wave in 2016. (a): Time series of area-averaged (35°-55°N; 11°W-15°E, see rectangle in panel (b)) daily maximum 2-metre temperature between 1 June and 30 September 2016. The green dashed line shows the daily ERA-Interim climatology for the reference period 1979-2016. Red filled area indicates the heat wave from 23 August to 16 September 2016. (b): Accumulated Heat Wave Magnitude Index daily (HWMId, Russo et al., 2015) values for the heat wave period.

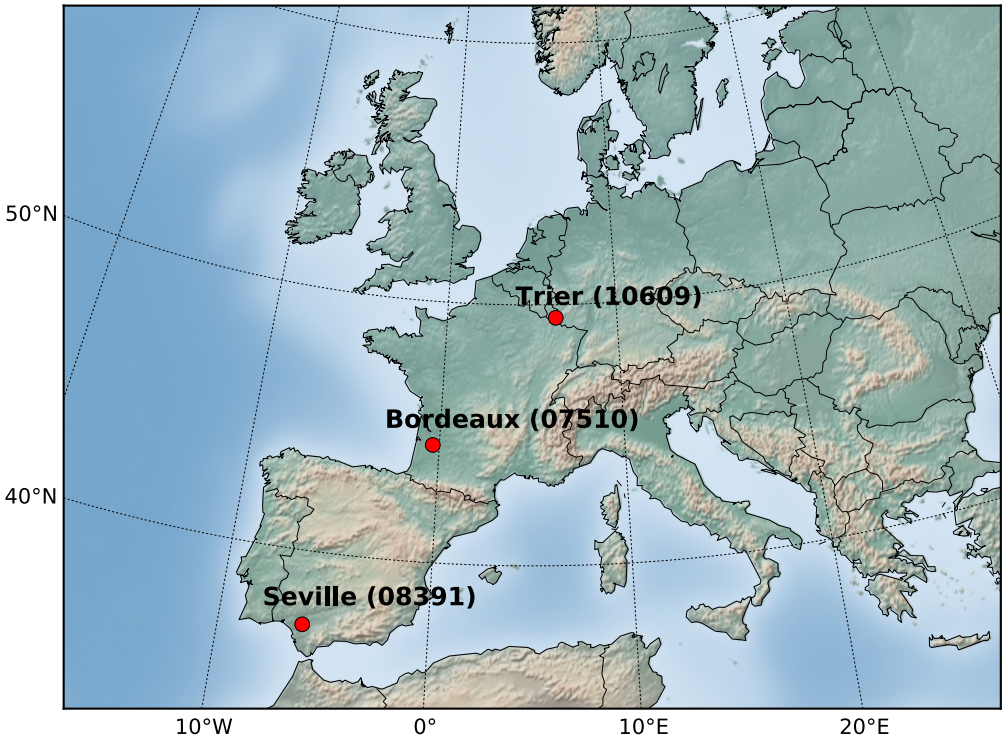

Figure 2. Geographical map of the investigated weather stations Bordeaux (France), Seville (Spain) and Trier (Germany) with WMO station numbers in parentheses.

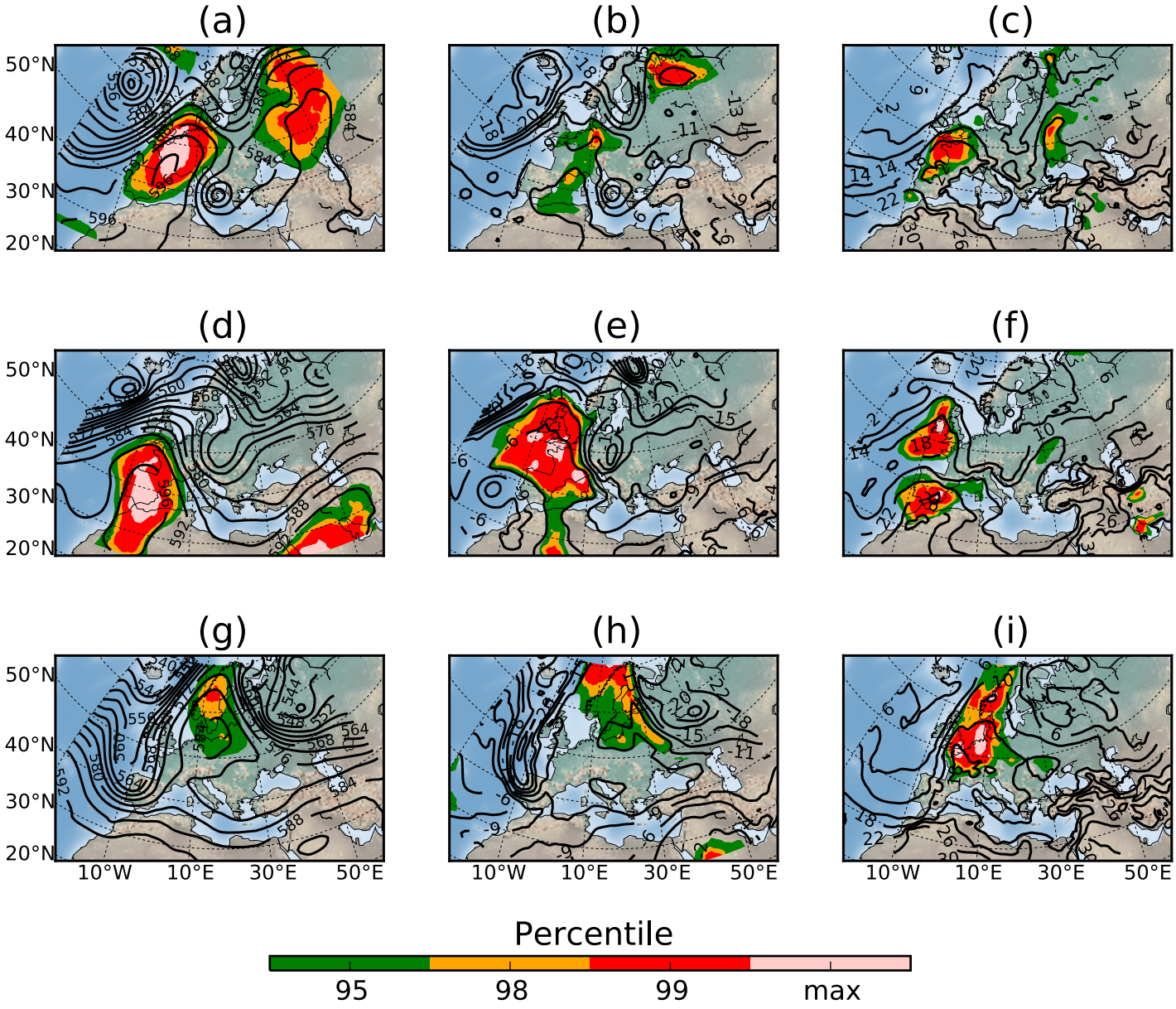

Figure 3. Synoptic overview for the three peaks during the heat wave. Left: Geopotential height at 500 hPa in gpdam. Middle: Temperature at 500 hPa in °C. Right: Temperature at 850 hPa in °C. These variables are contoured, areas exceeding the 95th, 98th, 99th percentiles and the highest value recorded in the reference period 1979-2016 are colour-shaded (see label bar). (a+b+c): 23 August 2016, (d+e+f): 5 September 2016 and (g+h+i): 13 September 2016.

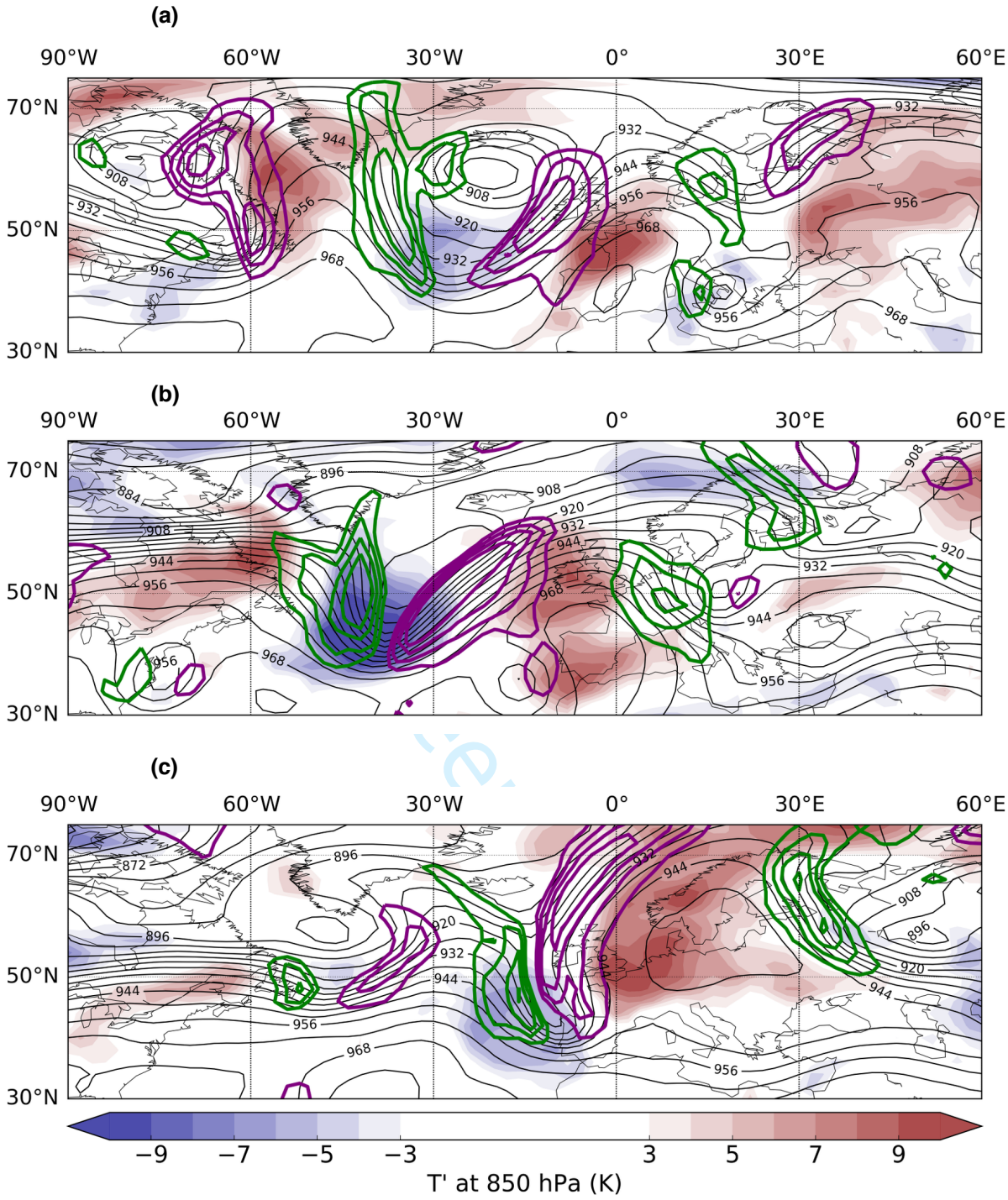

Figure 4. Relation of 300-hPa waviness and low-level temperature anomalies for the three peaks of the heat wave. Geopotential height (black contours, in gpdam) and meridional wind (contours, green: northerlies; purple: southerlies) isotachs starting at 20 m/s, then every 10 m/s. Coloured areas denote temperature anomalies at 850 hPa (reference period 1979-2016). (a) 23 August 2016; (b) 5 September 2016; and (c) 13 September 2016.

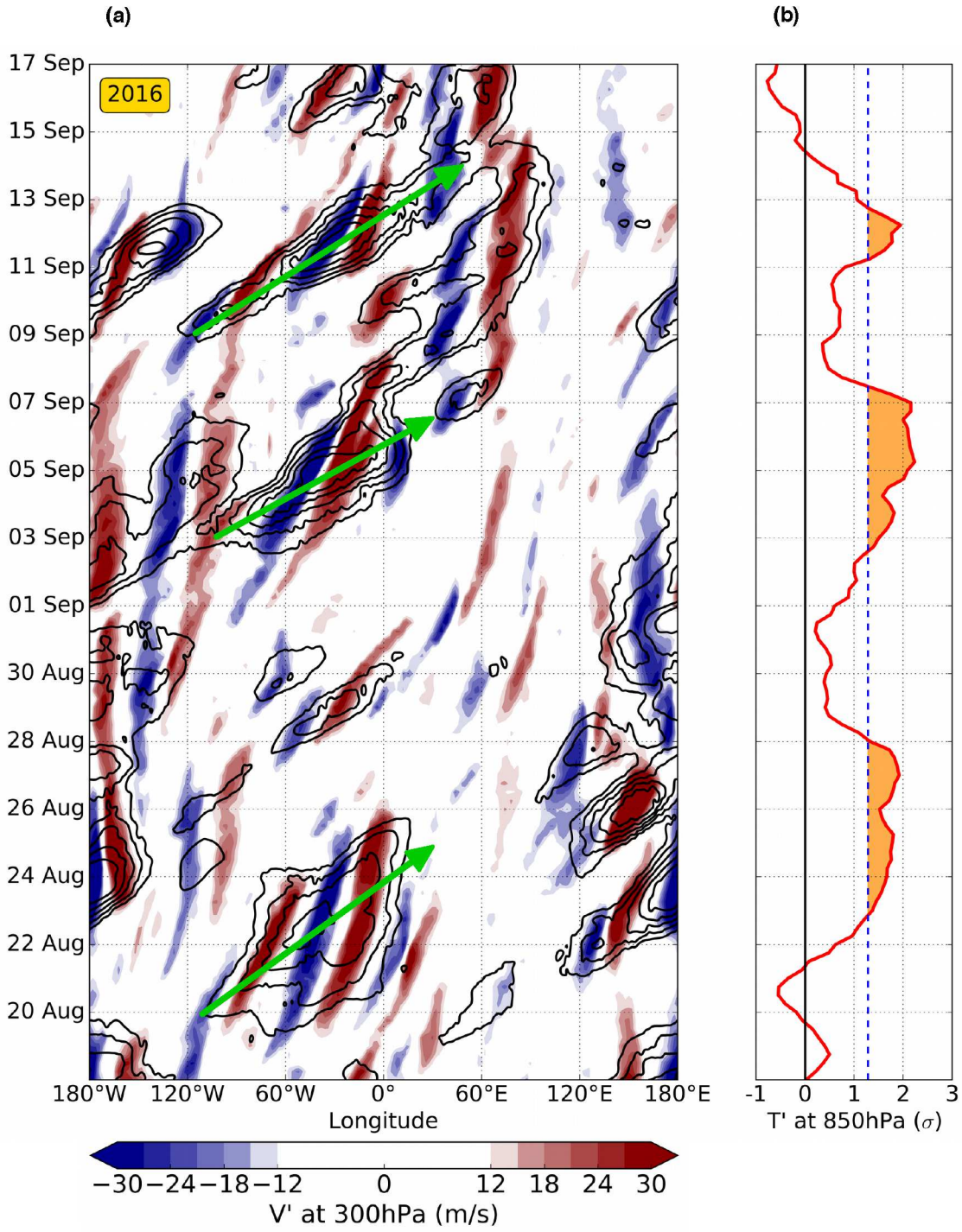

Figure 5. Hovmoeller diagram illustrating the upper tropospheric dynamics for the 2016 heat wave. The contours in (a) depict 300hPa RWP amplitude (in m/s, contours every 4 m/s from 22 to 38 m/s). A weak bivariate interpolation (using cubic Hermite splines) is applied to slightly smoothen the resulting field. In colour fill shown is the 300 hPa meridional wind anomaly (blue for northerlies and red for southerlies). The time resolution is 6-hours. Both fields were averaged over a 20° latitude band which self-adjusts (within the 30°N-70°N band) to those latitudes in which the highest RWP amplitudes occur. The green arrows approximate the group velocity of the eastward propagating RWPs. (b) Normalised temperature anomaly at 850 hPa (red line) averaged over 35°-55°N and 11°W-15°E (with a cos(latitude) weighting). Orange shading indicates that the temperature anomaly exceeds the 90th percentile for the months of August and September (blue dashed line).

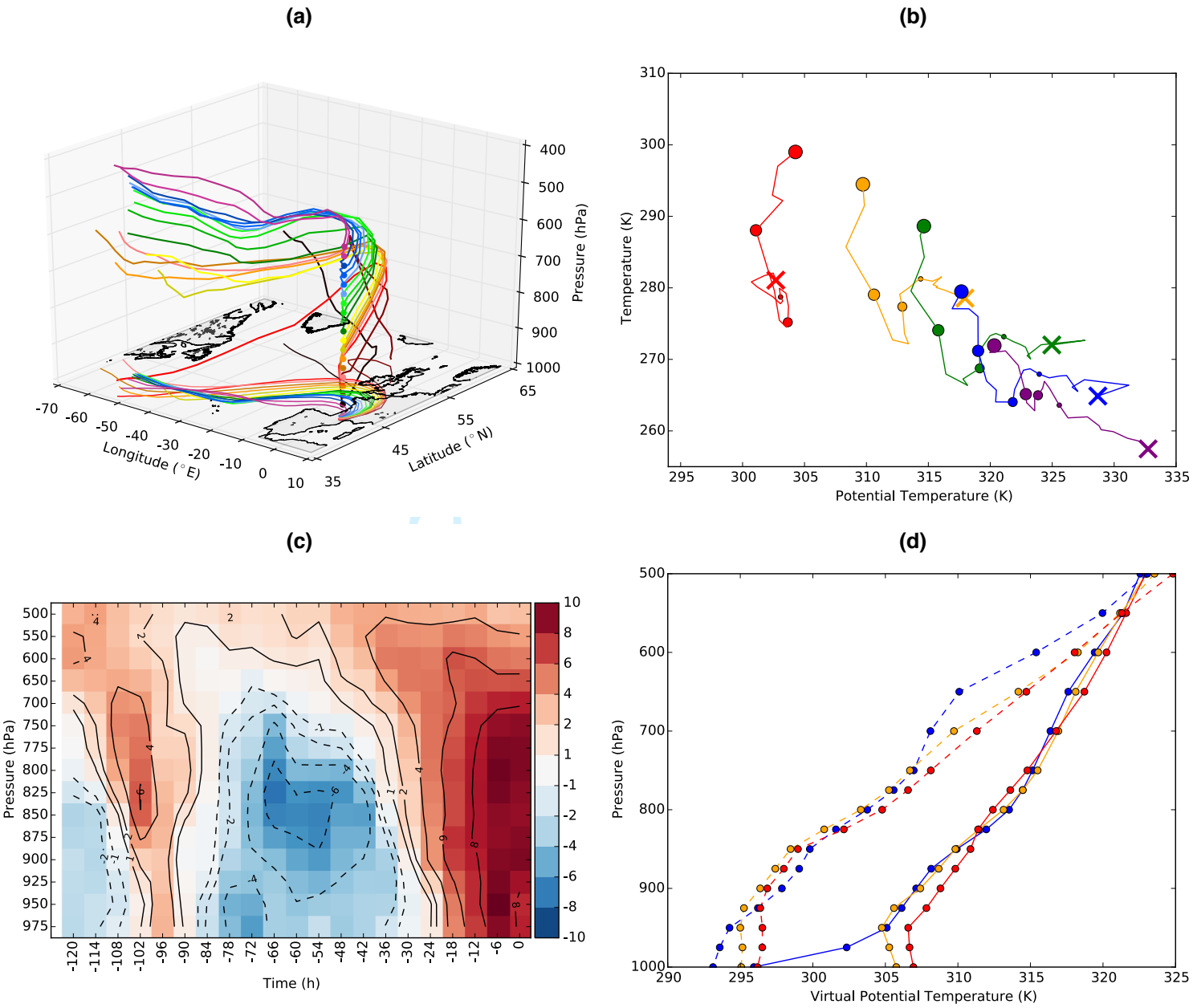

Figure 6. Lagrangian and Eulerian perspectives of the development of the peak of the heat wave in Bordeaux between 18 (1200 UTC) and 23 August 2016 (1200 UTC) (a): Three-dimensional representation of 5-day backward trajectories, started over Bordeaux between 975 and 550 hPa in 25 hPa increments. Only starting levels at which temperatures exceeded the 95th percentile on 23 August 2016 1200 UTC were taken. The surface position of the parcel is given on a two-dimensional map (bottom layer), with the colours indicating identical trajectories (black/reddish: 975-900 hPa, orange/yellowish: 875-800 hPa, greenish: 775-700 hPa, blueish: 675-600 hPa, purple: 575-550 hPa). (b): T-Θ diagram (cf. Box 1) showing the evolution of mean T and Θ of the trajectories in (a), grouped into 5 pressure levels that started over Bordeaux: 975-900 hPa (red), 875-800 hPa (orange), 775-700 hPa (green), 675-600 hPa (blue) and 575-550 hPa (purple). Decreasing size of filled circles represent 24-h intervals prior 23 August 2016, i.e. 0, 24, 48 and 72 h. The cross indicates the origin. (c): 6-hourly vertical temperature anomalies (base period 1979-2016, in °C) above Bordeaux for 18-23 August 2016. (d): Vertical virtual potential temperature profiles Θ_v for 18 (dashed, pre-heat wave) and 23 August (heat wave) at 0600 (blue), 1200 (orange) and 1800 UTC (red).

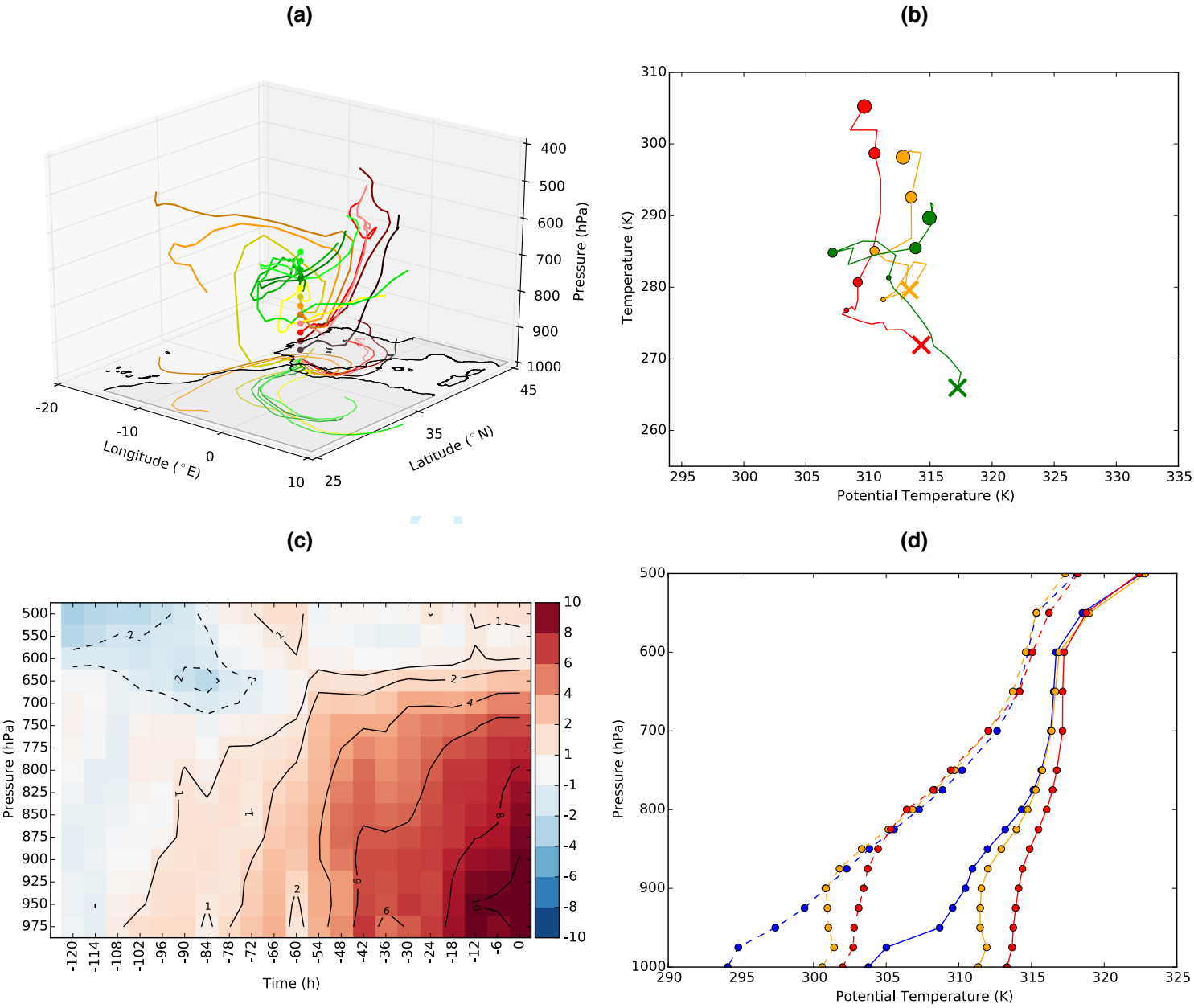

Figure 7. As in Fig. 5, but for Seville. Backward trajectories were started between 975 and 700 hPa and the 5-day period considered is between 31 August (1200 UTC) and 5 September 2016 (1200 UTC).

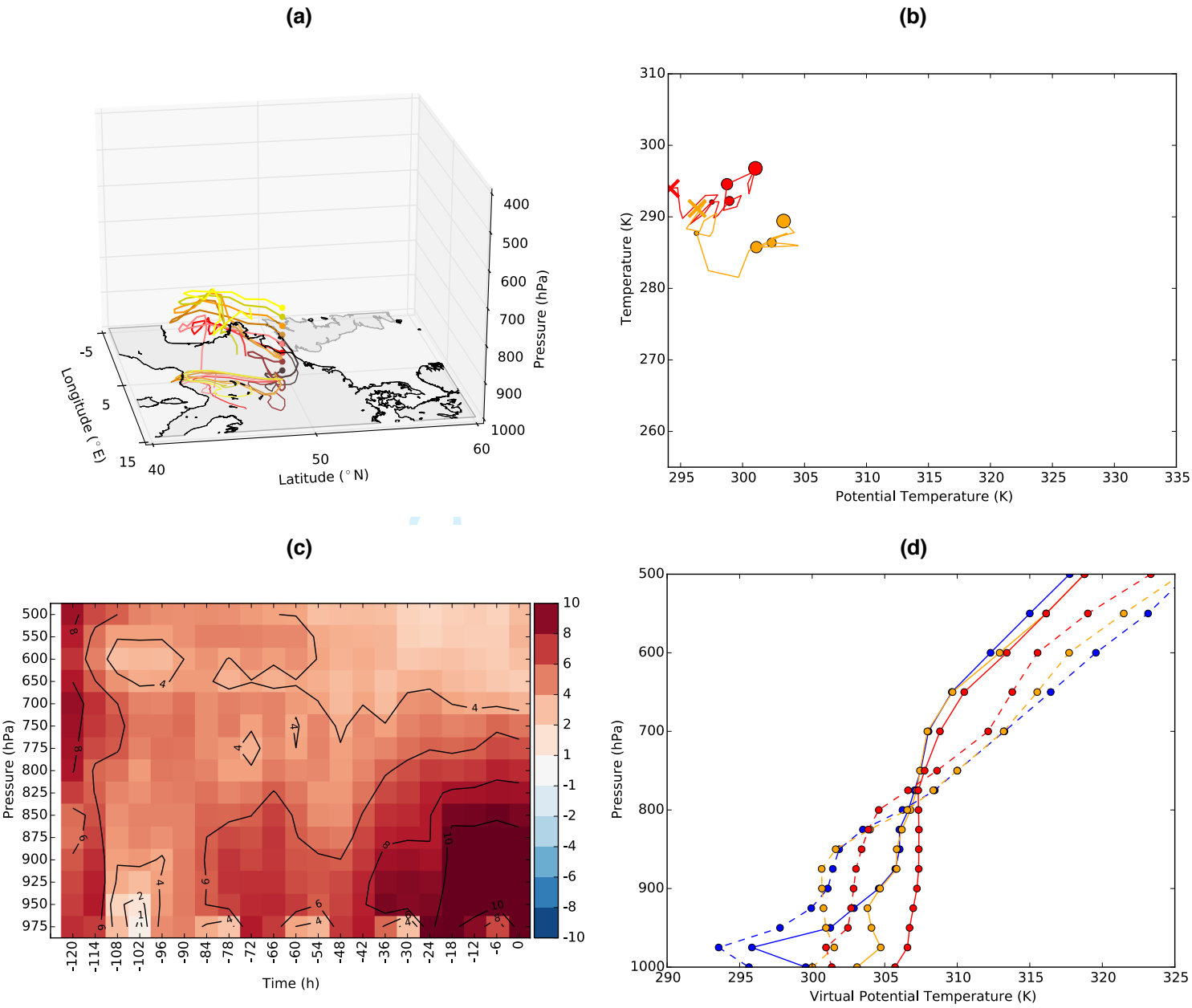

Figure 8. As in Fig. 5, but for Trier. Backward trajectories were started between 975 and 800 hPa and the 5-day period considered is between 8 (1200 UTC) and 13 September 2016 (1200 UTC).

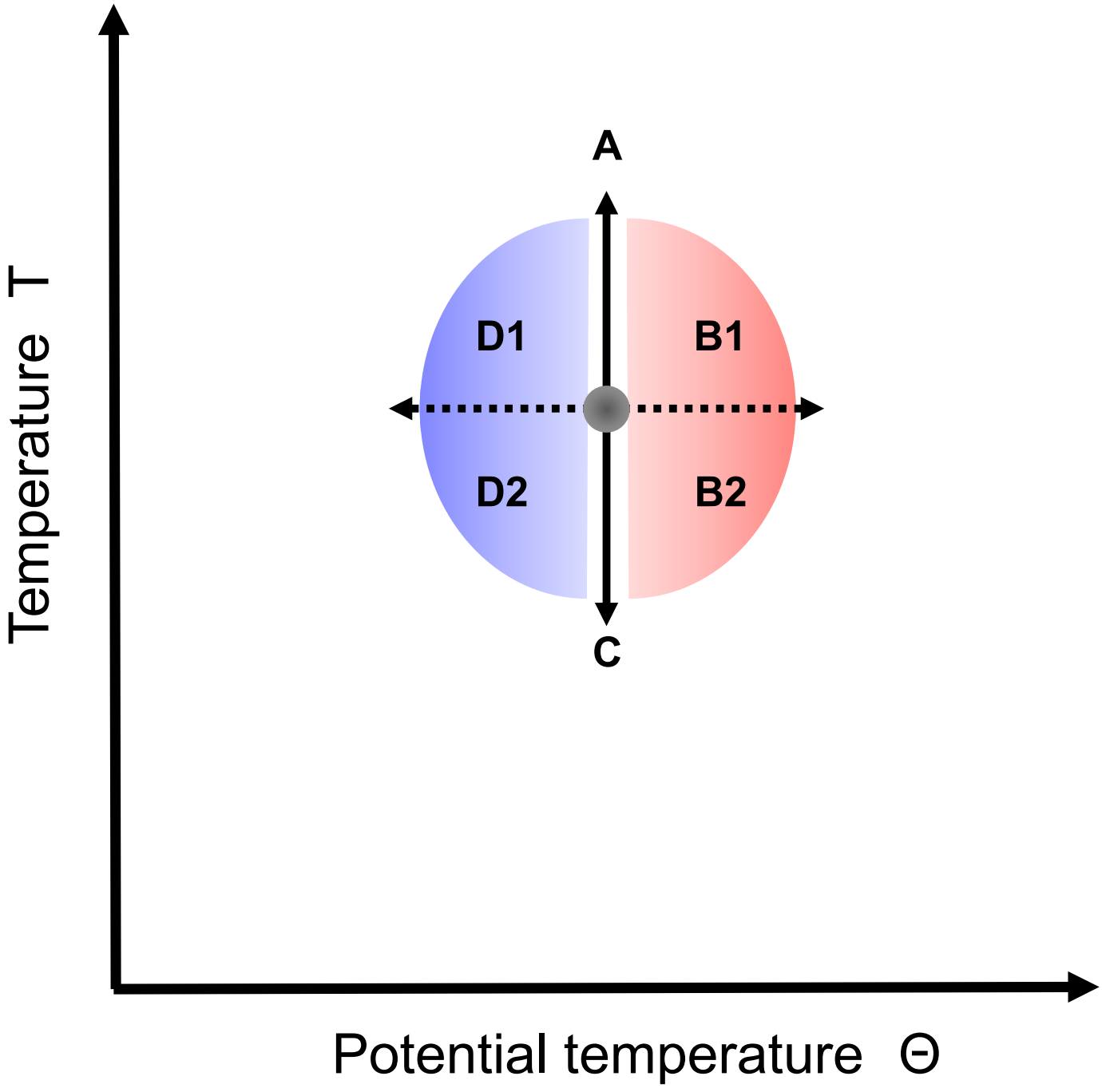

Scheme 1. T-Θ diagram.

Large-scale Rossby wave and synoptic-scale dynamic analyses of the unusually late 2016 heat wave over Europe

Philipp Zschenderlein[1*], Georgios Fragkoulidis[2], Andreas H. Fink[1], and Volkmar Wirth[2]

[1] Karlsruhe Institute of Technology, Institute of Meteorology and Climate Research, Karlsruhe, Germany

[2] Johannes Gutenberg University, Institute of Atmospheric Physics, Mainz, Germany

[*] Corresponding author: Philipp Zschenderlein, Karlsruhe Institute of Technology, Institute of Meteorology and Climate Research, Kaiserstr. 12, 76128 Karlsruhe, Germany. E-mail: philipp.zschenderlein@kit.edu

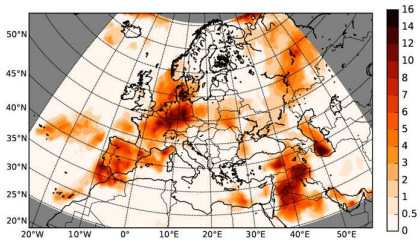

Graphical abstract

Parts of Europe were affected by a heat wave in the late summer of 2016 with record-breaking temperatures for this time of the year. The heat wave was associated with successive Rossby wave packets, which originated in western North America. During the heat wave, subsidence and ensuing adiabatic compression in the free atmosphere in combination with boundary layer processes rather than temperature advection were instrumental in the explanation of the extreme temperatures at the three selected surface stations.